JOURNAL OF THERMOPHYSICS AND HEAT TRANSFER
Vol. 22, No. 4, October–December 2008

Reactive Flow in Halide Chemical Vapor Deposition of Silicon Carbide Epitaxial Films

Rong Wang* and Ronghui Ma†
University of Maryland, Baltimore County, Baltimore, Maryland 21250

DOI: 10.2514/1.37729

Halide chemical vapor deposition emerges as a potent technique for growing silicon carbide epitaxial films at high deposition rates. Experimental studies suggest that thermal environment and fluid flow in the reactor are important factors that control the gas-phase and surface chemistry and therefore have a profound influence on the deposition rate, quality, and properties of the as-deposited films. In this study, a comprehensive transport model that includes gas dynamics, heat and mass transfer, gas-phase and surface chemistry, and radio-frequency induction heating is employed to study the complex heterogeneous chemical reactions as well as transport of multiple chemical species in a high-temperature environment. Simulations are performed over a wide range of operational parameters in a horizontal hot-wall reactor using $SiCl_4/C_3H_8/H_2$ as the precursors. The results show that deposition temperature and the flow rate of carrier gas are important factors determining the processing conditions and deposition rate. The model can be further used to improve reactor design and to optimize the processing conditions.

Nomenclature

$\mathbf{A}$	=	magnetic vector potential, Wb/m
D	=	mass diffusion coefficient, m^2/s
F	=	view factor
$\mathbf{g}$	=	gravitational acceleration, m/s^2
h	=	enthalpy, J/mol
$\mathbf{I}$	=	identity tensor
$\mathbf{I}_{\text{coil}}$	=	coil current, A
$\mathbf{J}_{\text{coil}}$	=	coil current density, A/m^2
K_T	=	thermal diffusion ratio
k	=	thermal conductivity, $W/m \cdot K$
k_s	=	rate constant of surface adsorption
M	=	molar mass, Kg/mol
N	=	total number of surfaces
N_{rt}	=	total number of reactions
N_{sp}	=	total number of species
p	=	pressure, Pa
q_j	=	rate-of-progress variable for jth reaction, $mol/m^3 \cdot s$
q'''_{eddy}	=	volumetric heating source induced by induction heating, W/m^3
q''_{radi}	=	surface radiative heat flux, W/m^2
R	=	universal gas constant, $J/K \cdot mol$
T	=	temperature, °C
$\mathbf{V}$	=	velocity, m/s
$[X]$	=	molar concentration of gaseous species, mol/m^3
Y	=	mass fraction
ε	=	surface emissivity
ε_m	=	relative electric permittivity
μ	=	viscosity, $Pa \cdot s$
μ_m	=	relative magnetic permeability
ν	=	stoichiometric coefficient
ρ	=	density of the gas mixture, kg/m^3
σ	=	Stefan–Boltzmann constant, $W/m^2 \cdot K^4$
σ_c	=	electric conductivity, $1/\Omega \cdot m$
ω	=	current frequency, Hz
$\acute{\omega}$	=	rate of species generation/consumption due to chemical reactions, $mol/m^3 \cdot s$

Subscripts

i	=	species index
j	=	reaction index, surface index
k	=	surface index

Superscripts

f	=	forward reaction
r	=	reverse reaction

Introduction

SILICON carbide (SiC) is an attractive semiconductor material for electronic devices working under extreme conditions such as high temperatures, high power, and erosive environments [1]. Recently, SiC has also found important applications for nano- and microelectromechanical systems because of its good thermal, mechanical, and chemical properties [2,3]. Currently, the most extensively employed technique for growing SiC epitaxial films is the chemical vapor deposition (CVD) method using silane (SiH_4) and propane (C_3H_8) highly diluted in hydrogen as precursors [4–9]. However, this method is not economically suitable for applications requiring thick SiC films (greater than 100 μm) due to its low deposition rate (3 to 15 μm/h). An alternative approach, halide chemical vapor deposition process (HCVD), is employed by several research groups to grow thick SiC films using chlorinated silicon-containing precursors such as silicon tetrachloride ($SiCl_4$), trichlorosilane ($SiHCl_3$), and methyltrichlorosilane (CH_3SiCl_3) [10–18]. Existing experimental studies suggest that the addition of chlorinated species leads to formation of $SiCl_2$. The good chemical stability and high surface activity of $SiCl_2$ at high temperatures allow the application of high deposition temperatures and high precursor flow rates in the HCVD process, leading to an elevated deposition rate in the range of 50–300 μm/h [13].

In the HCVD of SiC, the properties, quality, and deposition rates of the films are very sensitive to the processing conditions in the reactor, including thermal environment, gas flowfield, and chemical composition of the gas mixture. Previous experimental studies showed that increasing the deposition temperature leads to a decreased deposition rate [15]. In addition, manipulating the precursors' flow rates causes a substantial change in the film properties such as resistivity and doping level [12]. However, precise control of the film properties is difficult. Thus far, the growth

Received 25 March 2008; accepted for publication 12 June 2008.

*Ph.D. Candidate, Department of Mechanical Engineering.
†Assistant Professor, Department of Mechanical Engineering; roma@umbc.edu (Corresponding Author).

mechanism remains unclear, and the relationship between the processing conditions and film characteristics is not well understood. One challenge associated with the study of the HCVD process is that detailed information regarding the temperature distribution and chemical composition of the gas mixture in the vicinity of the substrate is not available. In situ measurement of the processing conditions (including temperature, gas velocity, and the concentrations of the chemical species) is severely limited by the high deposition temperature and erosive environment in the reactor.

Whereas numerical modeling has been extensively used as a means to study, design, and optimize a wide variety of vapor deposition processes, there is limited theoretical and numerical study on the HCVD of SiC. In our previous publication [19], we developed a comprehensive gas phase and surface reaction mechanism for the HCVD process using $SiCl_4/C_3H_8/H_2$. The reaction mechanism was integrated with a transport model that considers the gas flow and heat and mass transfer in a horizontal hot-wall reactor. The temperature and flowfields, the distributions of the gas species concentrations, and the deposition rate was predicted at various deposition temperatures. The predicted deposition rates agree well with the experimental measurements. However, this study only emphasized chemical kinetics and surface models; the impact of thermal and flow conditions on the deposition was not fully explored.

In this study, we have employed a multiphysics model for reactive flow in a HCVD system including gas-phase chemistry, surface kinetics, gas flow dynamics, mass and heat transfer, and radio-frequency induction heating to study the heterogeneous reactions in the gas phase and on the surface in a HCVD system. An order-of-magnitude analysis was conducted to characterize the main features of the process. Numerical simulations were performed to examine the effects of deposition temperature and carrier gas flow rate on the gas-phase composition and the deposition rate.

Simulation Configuration

A typical horizontal hot-wall HCVD reactor employed at Stony Brook University [14–16] is depicted schematically in Fig. 1. The SiC deposition occurs in a growth chamber that is made of a tubular dense graphite susceptor surrounded by graphite foam. A 6H-SiC substrate with the dimension of 1×1 cm is positioned on the inner wall of the susceptor. A mixture of gas precursors and carrier gas preheated to 50°C is delivered through a graphite channel from one end and exhausted from the other. The growth chamber is sealed in a double-walled, water-cooled quartz tube. The radio-frequency induction coils that surround the quartz tube are used to acquire the deposition temperature. The growth experiments were performed in the temperature range of 1400 to 1700°C at the pressure of 200 torr. The flow rates of $SiCl_4$, C_3H_8, and H_2 were in the range of 5–180 sccm, 2.5–30 sccm, and 5–15 slm, respectively [14–16]. In this study, the deposition temperature refers to the temperature at the center of the substrate.

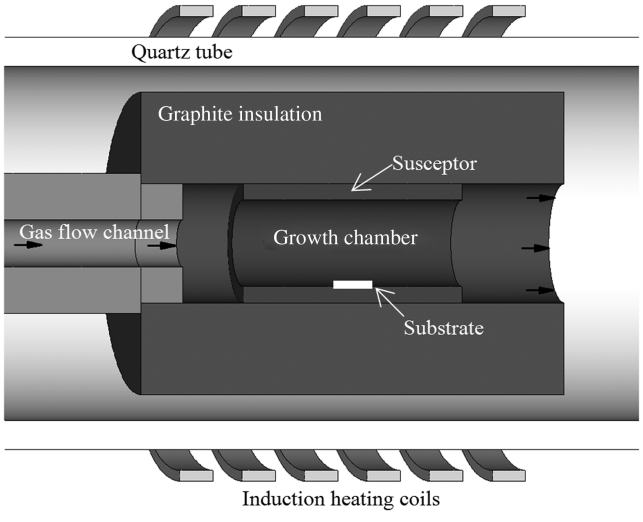

Fig. 1 Schematic of the hot-wall HCVD reactor used in this study [15].

Order-of-Magnitude Analysis

SiC deposition in the HCVD system involves complex transport phenomena, including gas flow, gas-phase and surface chemistry, transfer of multiple gas species, and conjugate modes of heat transfer by conduction, convection, and radiation. Order-of-magnitude analysis is employed in this study for characterizing the main features of the process. The values of main dimensionless numbers estimated for an H_2 flow rate of 5 slm are presented in Table 1. The Reynolds number for the deposition process performed over a temperature range of 1400 to 1700°C is evaluated to be 30 to 60. The magnitude of the Reynolds number indicates that the flow in the growth chamber is laminar. The Grashof number Gr, with a physical interpretation of the ratio of buoyancy forces to viscous forces, is very low, illustrating that the buoyancy-driven flow is weak in the process. The value of Schmidt number Sc, which represents the ratio of inertial momentum to mass diffusivity, varies in the range of 0.13–0.85 due to the largely different mass diffusivities of the gas species. The mass and thermal Peclet numbers are much higher than unity, suggesting that convection is the dominating process in the transfer of mass and energy. The surface Damköhler number is the ratio of the reaction rate of a species on the surface to its mass transport rate. Although a large Damköhler number indicates that the rate of deposition is controlled by mass transfer, a small Damköhler number suggests the deposition is limited by the rate of the reactions. For the growth conditions used in this study, the moderate Damköhler number (between 2.5–9) implies that the growth is controlled by both reaction kinetics and mass transport.

In current study, the exothermic/endothermic effect of chemical reactions is quantified by calculating the heat absorption/dissipation of major reactions. Through reviewing the chemical thermodynamic data of the reactions and the concentrations of the constituents in the gas mixture, the decomposition of $SiCl_4$ is identified as the most important chemical process that absorbs relatively substantial amount of heat in the gas phase when compared with other reactions in the system. Based on a $SiCl_4$ flow rate of 120 sccm and the deposition temperature of 1700°C, the heat absorption for the dissociation of $SiCl_4$ into $SiCl_2$ is calculated to be 0.52 W. The heat generation for film deposition at a typical deposition rate of 180 μm/h is estimated to be 0.001 W. In comparison with Joule heat induced in the dense graphite susceptor (1278 W), it is reasonable to neglect the exothermic/endothermic effect of the chemical reactions on temperature distribution in the growth chamber.

Mathematical Model

Radio-Frequency Induction Heating

Induction heating is applied in the HCVD system for achieving high deposition temperatures beyond 1400°C. The eddy current induced by the alternative current of high frequency through the coils generates Joule heat in the dense graphite susceptor, thus heating the system to a designated temperature. The magnitude and distribution of Joule heat are highly dependent on the reactor design and induction-heating system parameters such as frequency, coil geometry, input power, and the position of the coils in the axial direction. At a frequency less than 1 MHz, it is assumed that the electromagnetic field is quasi-steady and the current through the coils is time-harmonic. Thus, the distribution of the electromagnetic field is described by Maxwell's equation:

$$\nabla \times \left(\frac{1}{\mu_m} \nabla \times \mathbf{A}\right) + \varepsilon_m \frac{\partial^2 \mathbf{A}}{\partial t^2} + \sigma_c \frac{\partial \mathbf{A}}{\partial t} = \mathbf{J}_{\text{coil}} \tag{1}$$

The current model considers the magnetic vector potential to be diminished at the infinite distance from the induction coils:

Table 1 Dimensionless numbers for the HCVD process (H_2 flow rate: 5 slm)

Temperature	T, °C	1400–1700
Density	ρ, kg/m^3	1.24×10^{-2}–1.70×10^{-2}
Thermal conductivity	k, W/m K	0.63–0.74
Heat capacity	C_p, J/kg K	1.58×104–1.66×104
Mass diffusivity	D, m^2/s	2.00×10^{-3}–1.00×10^{-2}
Velocity	V, m/s	1.50–2.00
Characteristic length	d, m	0.04
Kinematic viscosity	$\nu = \mu/\rho$, m^2/s	1.32×10^{-3}–2.04×10^{-3}
Thermal diffusivity	$\alpha = k/\rho C_p$, m^2/s	2.35×10^{-3}–3.57×10^{-3}
Reynolds number	$Re = Vd/\nu$	30–60
Grashof number	$Gr = \rho^2 g \beta d^3 \Delta T/\mu^2$	70–200
Schmidt number	$Sc = \nu/D$	0.13–0.85
Prandtl number	$Pr = \nu/\alpha$	0.37–0.87
Peclet number (mass)	$Pe_{\text{mass}} = Re \cdot Sc$	4–51
Peclet number (thermal)	$Pe_{\text{therm}} = Re \cdot Pr$	11–52
Surface Damköhler number (Si species)	$Da = k_s d/D$	2.5–9

$$A = 0 \quad \text{as} \quad r^2 + z^2 \to \infty \tag{2}$$

This boundary condition is applied by using a very large computational domain. Initially, a moderate-sized domain is used. The size of the domain is then increased progressively until it does not affect the magnetic field distribution. The volumetric Joule heating power induced by the eddy current is calculated using Joule's law:

$$q'''_{\text{eddy}} = \tfrac{1}{2}\sigma_c \omega^2 |\mathbf{A}|^2 \tag{3}$$

Joule heat induced in the susceptor is implemented in the model for energy transport to solve for the temperature distribution in the reactor.

Transport Processes

The fluid flow, heat, and mass transfer in a HCVD reactor are governed by the conservations of mass, momentum, thermal energy, and individual species. Based on the order-of-magnitude analysis, we assume that the film grows at steady state, the flow is laminar, the gas mixture is ideal gas, and the viscous dissipation of the gas mixture is negligible. In a multicomponent system, the presence of a temperature gradient can give rise to a diffusion flux due to the Soret effect [20]. Previous modeling work of SiC CVD in cold-wall and hot-wall reactors [5,9] showed that thermal diffusion, which causes large molecules to move toward the cold region and small molecules to move toward the hot region, has substantial influence on the film growth. Thereby, the effect of thermal diffusion is also considered in this model. The exothermic/endothermic effect of the chemical reactions is not considered in this model based on the order-of-magnitude analysis. The transport of momentum, energy, and mass in a reactor is described by the following equations:

$$\nabla \cdot (\rho \mathbf{V}) = 0 \tag{4}$$

$$\rho \mathbf{V} \cdot \nabla \mathbf{V} = -\nabla p + \nabla \cdot \{\mu[\nabla \mathbf{V} + (\nabla \mathbf{V})^T] - \tfrac{2}{3}\mu \mathbf{I} \nabla \cdot \mathbf{V}\} + \rho \mathbf{g} \tag{5}$$

$$\nabla \cdot (\rho \mathbf{V} h) = \nabla \cdot (k \nabla T) + q'''_{\text{eddy}} + \nabla \cdot q''_{\text{radi}} \tag{6}$$

$$\nabla \cdot (\rho \mathbf{V} Y_i) = \nabla \cdot \{\rho D_i [\nabla Y_i + K_{Ti} \nabla (\ell_n T)]\} + \dot{\omega}_i \tag{7}$$

where $\dot{\omega}_i$ is calculated from the kinetic chemical reaction mechanism, and q''_{radi} is the radiative heat flux on the surfaces of the inner enclosure of the growth chamber calculated using the integrodifferential radiative heat transfer equation [16]:

$$\frac{q''_{\text{radi},j}}{\varepsilon_j} - \sum_{k=1}^{N} F_{j,k} \frac{1 - \varepsilon_k}{\varepsilon_k} q''_{\text{radi},k} = \sigma T_j^4 - \sum_{k=1}^{N} F_{j,k} \sigma T_k^4 \tag{8}$$

Because of the temperature difference present in the HCVD system, the temperature-dependency of the physical properties of the gas species is addressed in this study. The density of the gas is determined as a function of temperature and pressure using the ideal-gas law:

$$p = \rho R T \sum \frac{Y_i}{M_i} \tag{9}$$

Under typical deposition conditions, the flow rate of carrier gas H_2 is much higher than that of C_3H_8 and $SiCl_4$. Hence, the gas mixture is considered to be highly dilute, and binary diffusion coefficients of the gas species in hydrogen are used in Eq. (7). The binary diffusion coefficients are calculated based on the gas molecular theory [20]. We use commercial software CHEMKIN to evaluate the binary diffusivity D_i of the gas species in hydrogen [21]. Other temperature-dependent gas properties such as thermal conductivity and viscosity are also taken from the same database.

Because the growth chamber is situated in a quartz tube that is cooled by circulating water during the film growth, the outer boundary of the computational domain is assumed to be at room temperature. At the entrance of the gas delivery channel, a constant velocity is applied to satisfy the flow rates of the carrier gas and the precursors. Our calculation shows that the hydrodynamic entrance length in the gas delivery channel is around 1.6 cm for the processing conditions used in this study. Thus, the precursor gas flow is considered to be fully developed in the gas delivery channel before entering the growth chamber. The gas temperature is preheated to 50°C before entering the system. A constant pressure of 200 torr is applied at the outlet of the growth chamber.

Gas-Phase and Surface Reaction Kinetics

In our previous study [19], a comprehensive kinetic reaction mechanism for SiC growth from $SiCl_4/C_3H_8/H_2$ was proposed, including gas-phase and surface reactions. The proposed gas-phase reactions consist of one set of reactions for C_3H_8 decomposition, one set for $SiCl_4$ decomposition, and one set for the reactions among products from the first two sets in a hydrogen environment. The gas-phase reaction mechanism involves 33 gas species and 76 reactions. The surface deposition model involves nine surface species and 29 reactions that describe the kinetics of gas species adsorption, surface reactions, film etching by HCl, and film formation. Particularly, the effects of the available surface sites of Si and C on the vapor/solid interface are taken into consideration. The formation of surface structure, which requires simulation of the activities of Si and C

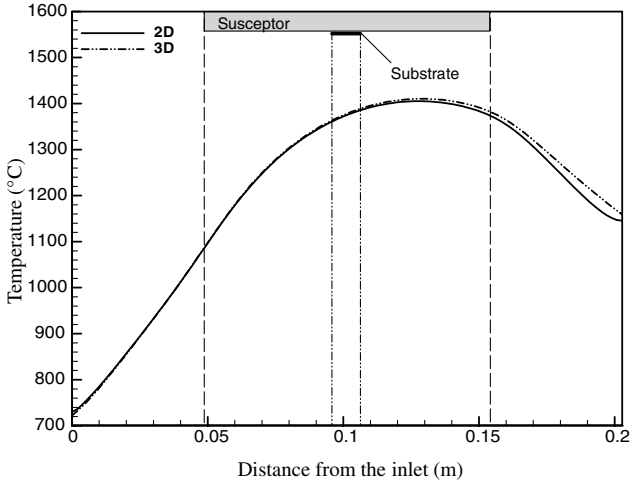

a)

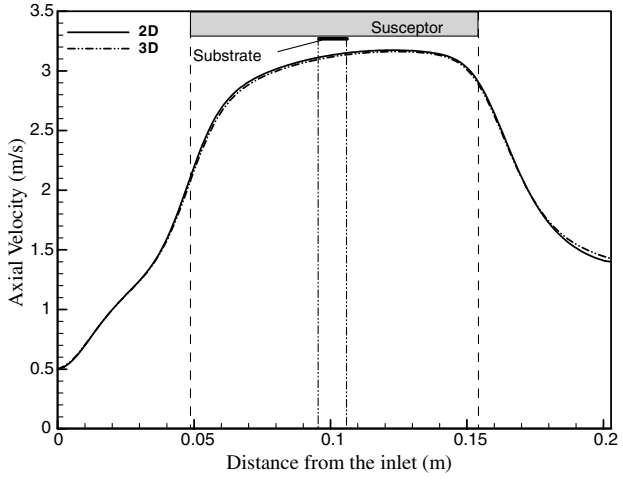

b)

Fig. 2 Comparison of 2-D and 3-D simulations: a) temperature profiles and b) axial velocity profiles along the reactor axial centerline.

atoms on the vapor/solid interface at atomic level, is not considered in this study.

In the gas phase, the rate of production or consumption of each species, $\dot{\omega}_i$, due to chemical reactions is calculated as follows [22]:

$$\dot{\omega}_i = \sum_{j=1}^{N_{rt}} v_{ij} q_j \tag{10}$$

The rate-of-progress variable for the jth reaction, q_j, is defined as

$$q_j = (k^f)_j \prod_{i=1}^{N_{sp}} [X_i]^{v'_{ij}} - (k^r)_j \prod_{i=1}^{N_{sp}} [X_i]^{v''_{ij}} \tag{11}$$

where $(k^f)_j$ and $(k^r)_j$ are the forward and reverse rate constants for the jth reaction, respectively. They are defined by Arrhenius law:

$$k_j = A_j T^{n_j} \exp\left(-\frac{Ea_j}{RT}\right) \tag{12}$$

where A_j, n_j, and Ea_j are Arrhenius kinetic parameters. The detailed kinetic data for the gas-phase and surface reactions can be found in our previous publication [19].

Computational Issues

The distributions of gas velocity, temperature, and species' concentrations in the reactor chamber are determined through solving the equations of electromagnetic dynamics, reaction kinetics, and conservations of energy, momentum, and individual mass species. A three-dimensional simulation that involves complex gas-phase and surface kinetic calculation means protracted computational time. Based on the order-of-magnitude analysis, the ratio of Grashof number to Reynolds number square, Gr/Re^2, with a physical interpretation of the ratio of buoyancy forces to inertial forces, is evaluated to be 0.05–0.09. The low value of Gr/Re^2 implies that the flow is dominated by forced convection. If the buoyancy-driven flow can be neglected, the configuration of the reactor allows for the assumption of axisymmetry, and the 2-D model can be implemented to save computational time. To validate this assumption, both 2-D and 3-D models are used to simulate the gas flow and temperature distribution in the reactor at the deposition temperature of 1500°C and pressure of 200 torr. A comparison of the 2-D and 3-D results is shown in Fig. 2. It is evident that the influence of buoyancy on the velocity field and temperature distribution is negligible. Therefore, the simulations presented in this study were performed with the assumption of axisymmetry. Although 2-D simulation has the limitations of addressing the effect of buoyancy-induced flow and uniformity of the deposition, it provides an expedient means of studying the kinetics of gas-phase and surface chemistry.

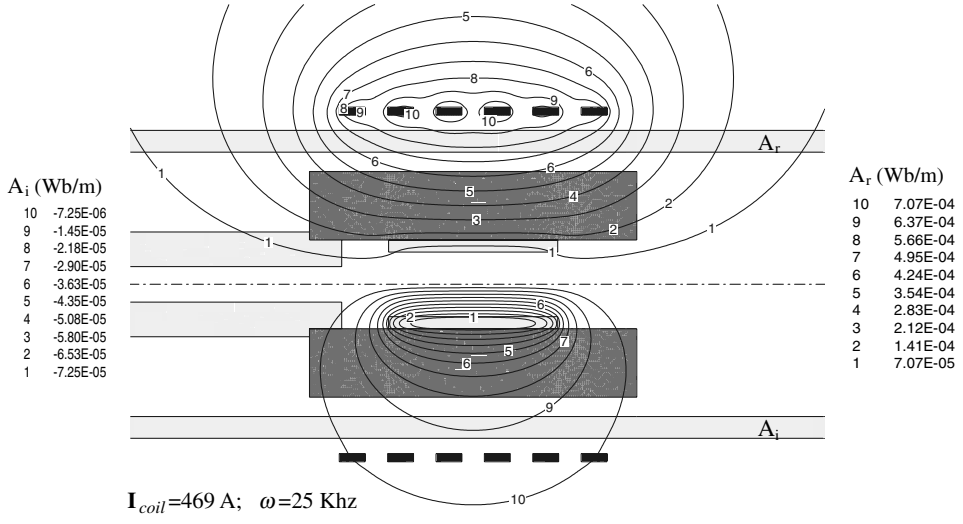

Fig. 3 Distributions of in-phase (A_r) and out-of-phase (A_i) components of the azimuthal magnetic vector potential.

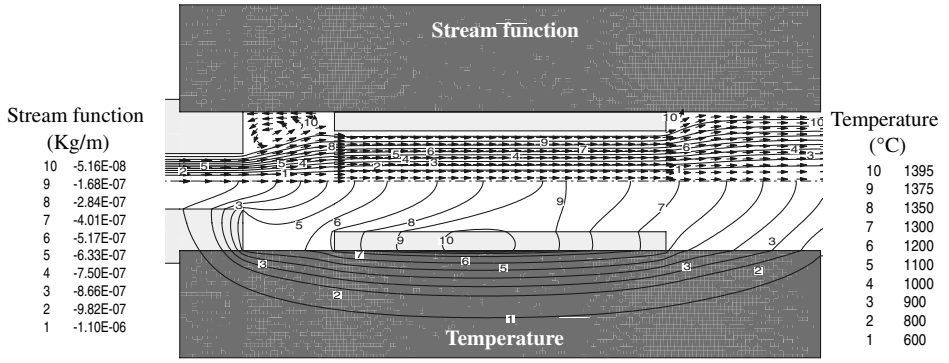

Fig. 4 Flowfield and temperature distributions in the reactor.

The simulations are performed using the commercial software package CFD-ACE with a mesh system of 349×133. The grid dependence of the results has been examined using a refined grid system and consistent results have been produced.

Results and Discussions

In the HCVD process, the decomposition of the precursors and the reactions among the products lead to the film growth on the substrate. The deposition rate is determined by surface reaction kinetics as well as the rates at which the reacting species are transported to the substrate surface. In this paper, simulation results are presented to illustrate the effects of the growth temperature and the carrier gas flow rate on the chemical composition of the gas mixture and the deposition rate.

Flowfield and Temperature Distribution

The distribution of the electromagnetic field at a frequency of 25 KHz and a current of 469 A is presented in Fig. 3 in terms of the azimuthal component of the magnetic vector potential. Shown in Fig. 4 is the corresponding temperature distribution and flowfield in the reactor when the hydrogen flow rate is 5 slm. Because of the high electric conductivity of the dense graphite, heat is mainly induced in the susceptor and the highest temperature is observed in the vicinity of the substrate. Figure 5 shows the dependence of temperature at the center of the substrate on the current passing through the coils at various H_2 flow rates. The deposition temperature is observed to be increasing linearly with the coil current. Figures 6a and 6b present the temperature profiles along the axial centerline of the growth chamber and on the susceptor surface for the deposition temperatures ranging from 1400 to 1700°C and an H_2 flow rate of 5 slm, respectively. It shows that the gas mixture was heated substantially in the gas delivery channel before being introduced into the growth chamber. The gas temperature is then increased rapidly by convection between the gas and the susceptor. In addition to convective heat transfer, radiation from the susceptor to the surrounding is very strong at high temperatures, as evidenced by the large temperature gradient in the axial direction. The presence of the graphite channel in front of the growth chamber reduces the radiation exchange between the susceptor and the surrounding. As a result, the temperature on the susceptor surface in the front region is higher than that in the rear, despite the fact that the upstream gas flow has a lower temperature than the downstream flow.

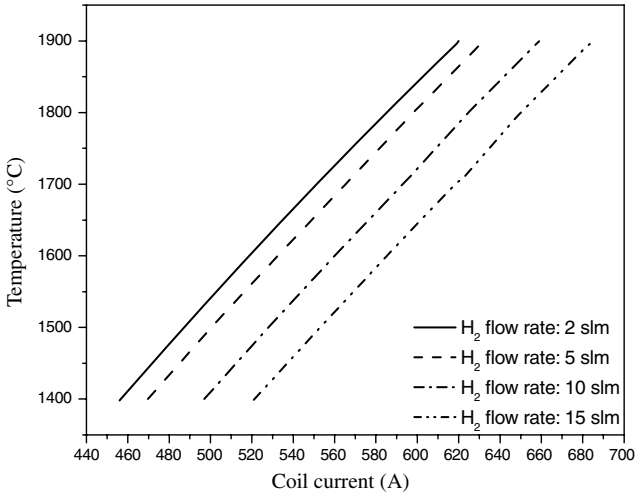

Fig. 5 Variations of the deposition temperature with the coil current.

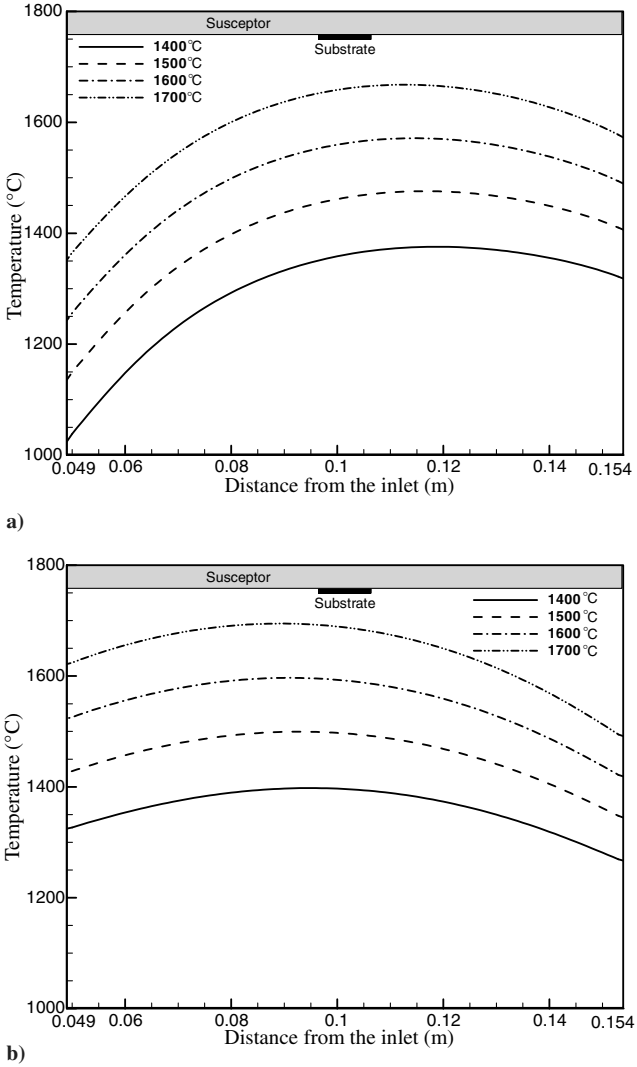

Fig. 6 Temperature profiles a) along the reactor axial centerline and b) on the susceptor surface.

Gas-Phase Composition

Once the gas mixture enters the growth chamber, chemical reactions occur in the gas phase and on the surface of the substrate. The chemical composition of the gas mixture and the deposition rate of the film are dependent on the thermal environment, flow conditions, and kinetics of the reactions. Although 33 gas species are considered in the reactor, not all of them have a concentration high enough to influence the growth substantially. Shown in Fig. 7 are the molar concentration profiles of main species along the reactor axial centerline at the growth temperature of 1400°C when $SiCl_4$, C_3H_8, and H_2 flow rates are 120 sccm, 10 sccm, and 5 slm, respectively. Because the rates of the chemical reactions are highly temperature-dependent, the concentration distributions of the gas species are not uniform. It suggests that the precursor gas C_3H_8 and $SiCl_4$ decompose very fast after entering the system, producing important Si- and C-containing species, including $SiCl_2$, SiCl, $SiHCl_3$, CH_4, and CH_3. Among these species, $SiCl_2$ and CH_4 have the highest concentrations. Figure 8 depicts the concentration distributions of CH_4 and $SiCl_2$ in the reactor chamber for a deposition temperature of 1400°C and a carrier gas flow rate of 5 slm.

An important feature worth noticing in Fig. 7 is the abundance of HCl present in the growth chamber. The study of the surface chemistry involved in HCVD of SiC by La Via et al. [10] and Veneroni and Masi [11] suggests that HCl is an active etching agent on the SiC surface and has an appreciable impact on deposition due to its high concentration. The corresponding reaction is $SiC(B) + HCl \rightarrow SiCl(S) + CH(S)$, where B and S represent bulk phase and surface species, respectively. The HCl in the current system is mainly formed by the reaction of chloride atoms with hydrogen: $H_2 + Cl \leftrightarrow HCl + H$, where chloride atoms are produced as $SiCl_4$ dissociates into $SiCl_2$ and SiCl. Therefore, the concentration of HCl is determined by many factors, including the flow rates of $SiCl_4$ and H_2, the temperature in the growth chamber, and the method by which the gas is delivered.

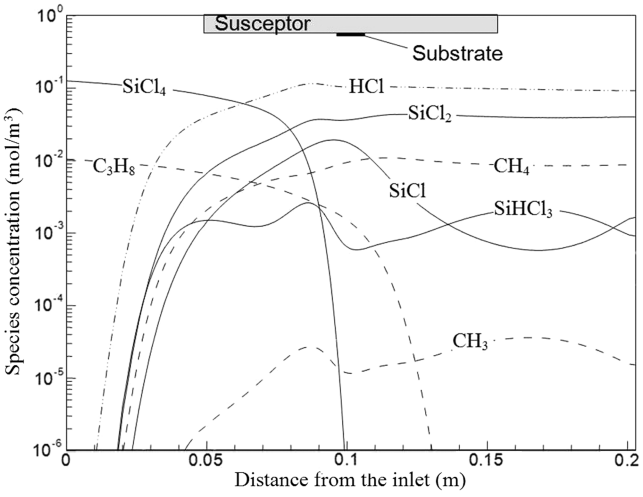

Fig. 7 Molar concentrations of main species along the axial centerline of the reactor.

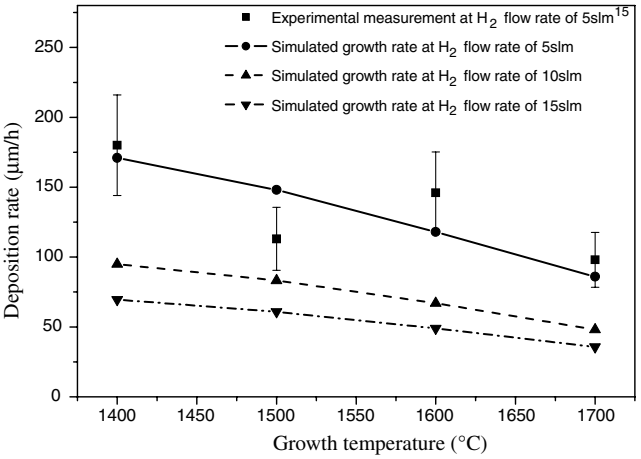

Fig. 9 Predicted deposition rates at various growth temperatures and H_2 flow rates.

Effect of Temperature on the Deposition Rate

The growth of SiC films was modeled at the deposition temperatures ranging from 1400 to 1700°C, with the flow rates of $SiCl_4$ and C_3H_8 being 120 and 10 sccm, respectively. Three flow rates of hydrogen (5, 10, and 15 slm) were applied to examine the effects of carrier gas flow rate on the deposition rate. The predicted film growth rate agrees reasonably well with the experimental measurements under identical processing conditions [15]. Further, as shown in Fig. 9 the numerical prediction captures the decreasing trend of the deposition rate with increasing temperature, as predicted by the thermodynamic equilibrium analysis and experimental growth [14]. The reduced deposition rate with temperature can be explained by the etching of SiC film by HCl at higher temperatures. Shown in Fig. 10 is the HCl concentrations on the substrate surface at different deposition temperatures for different H_2 flow rates. It shows that HCl concentration remains nearly constant at different temperatures. However, the rate constant of the etching reaction is reported to increase sharply with temperature [11]. Therefore, although high temperatures facilitate film deposition, the HCl etching overrides the surface reactions at these temperatures and leads to compromised deposition rates. Figure 9 also suggests that increasing the hydrogen flow rate results in a reduced deposition rate. The effects of temperature on the deposition rate are less obvious at elevated H_2 flow rates, because the higher carrier gas flow rate dilutes the concentration of HCl and mitigates the etching effect.

Effect of Carrier Gas Flow Rate

The flow rate of the carrier gas is an important operational parameter that affects the flowfield, temperature distribution, rate of mass transport, and residence time of the gas species in a growth

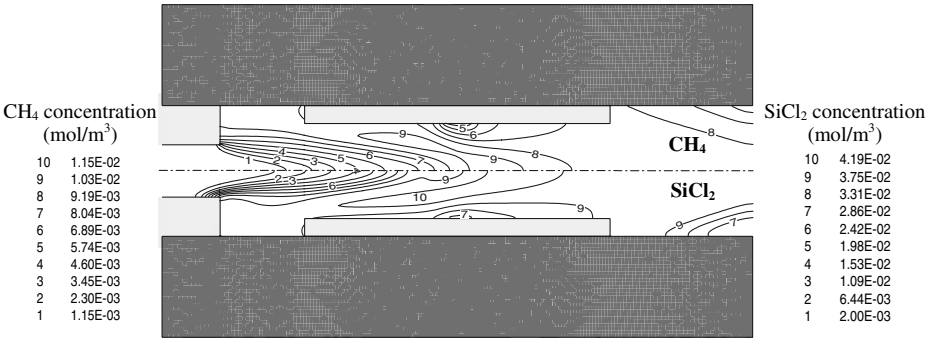

Fig. 8 CH_4 and $SiCl_2$ concentration distributions in the reactor.

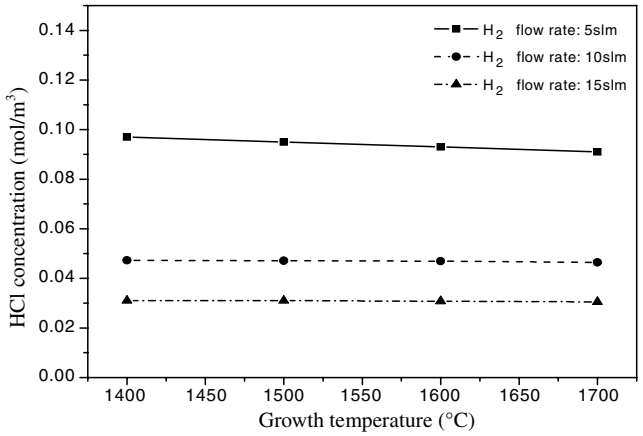

Fig. 10 HCl concentrations on the substrate at various growth temperatures and H_2 flow rates.

chamber. For the HCVD of SiC films, the carrier gas H_2 is also actively involved in the gas-phase and surface reactions. To study the effect of H_2 flow rate on the deposition, we performed numerical experiments with three different H_2 flow rates: 5, 10, and 15 slm at various deposition temperatures. For each of the temperatures, the power of the induction-heating device was adjusted so that the deposition temperature at the center of the substrate remained unchanged. At the deposition temperature of 1400°C, the Reynolds

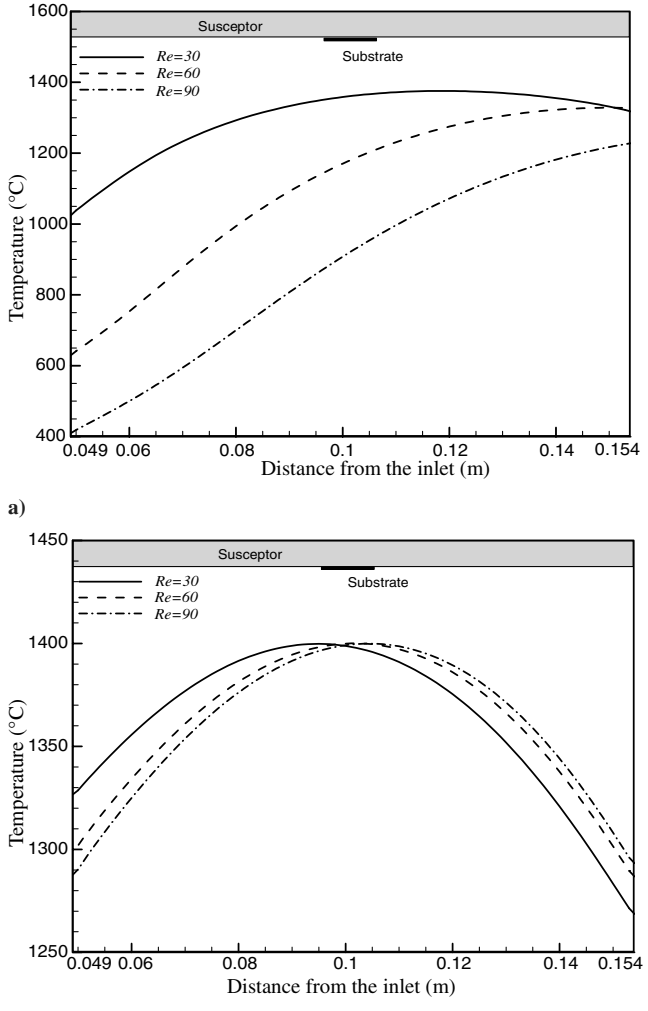

Fig. 11 Temperature profile a) along the axial centerline of the reactor and b) on the susceptor surface for various H_2 flow rates.

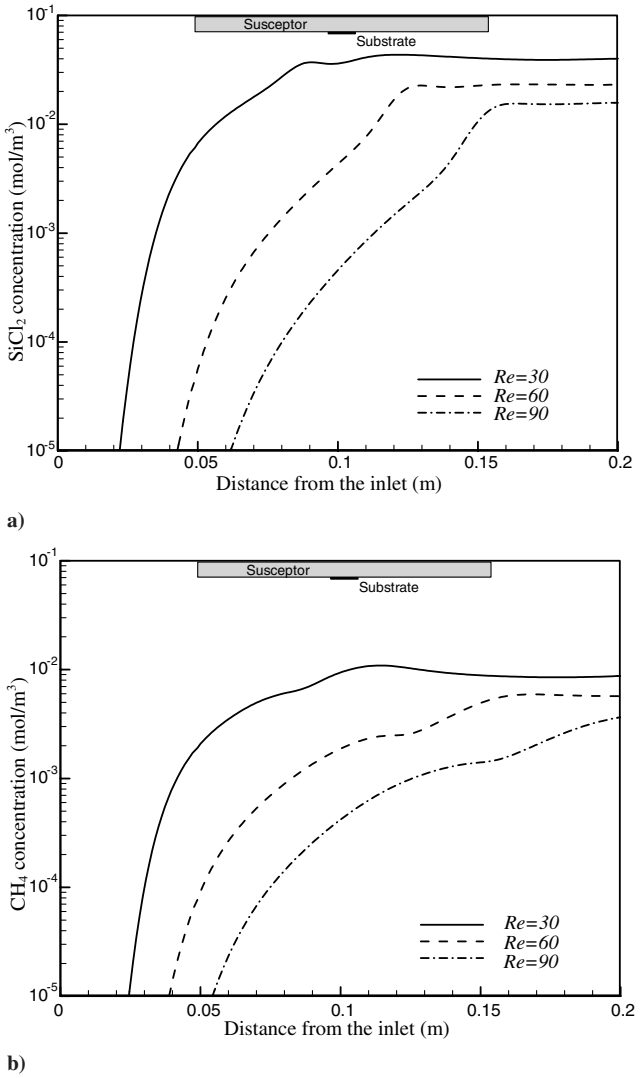

Fig. 12 Concentrations of a) $SiCl_2$ and b) CH_4 along the axial centerline of reactor for various H_2 flow rates.

numbers for H_2 flow rates of 5, 10, and 15 slm are 30, 60, and 90, respectively. Figures 11a and 11b show the temperature profiles along the axial centerline of the growth chamber and on the susceptor surface, respectively. It is evident that the enhanced flow rate of H_2 reduces the gas temperature considerably while enlarging the temperature gradient from 60 to about 100°C/cm along the axial centerline of the growth chamber. Because chemical reactions are sensitive to temperature, a decreased reaction rate in the gas phase is anticipated at higher H_2 flow rate. On the other hand, the influence of the H_2 flow rates on the temperature at the susceptor surface is less obvious. Figures 12a and 12b show, respectively, the concentrations of $SiCl_2$ and CH_4 along the axial centerline of the growth chamber at the deposition temperature of 1400°C for various H_2 flow rates. Because of the elevated carrier gas flow rate and the decrease in the temperature of the gas mixture, substantially reduced concentrations of main reacting species $SiCl_2$ and CH_4 are observed. Although increasing carrier gas flow rate will enhance mass transport through the boundary layer to the substrate, the resulting low concentrations of the main reacting species and reduced residence time cause decreased deposition rates, as evidenced in Fig. 9. The substantial effect of H_2 on the deposition process suggests that the H_2 flow rate must be selected carefully to achieve the desired deposition rate.

Conclusions

A comprehensive model of the SiC HCVD system using $SiCl_4/C_3H_8/H_2$ as precursors has been developed and applied to a

horizontal hot-wall reactor to study the reactive flow and the deposition of SiC films. Specifically, the effects of deposition temperature and carrier gas flow rate are examined. The predicted chemical composition of gas mixture suggests a high concentration of HCl in the growth chamber, which causes etching of the film. The reduced deposition rates at elevated temperatures are explained as the result of enhanced etching by HCl. The simulation of deposition at various H_2 flow rates also shows that the carrier gas flow rate can significantly affect the thermal field, rate of chemical reactions, and the species concentrations, thereby leading to largely different deposition rates. The model developed in this study can be further used to design processing conditions and reactor geometries that favor the deposition of the films at a controlled rate.

Acknowledgment

The authors would like to acknowledge Michael Dudley from Stony Brook University for valuable discussions and for providing the dimensions of the chemical vapor deposition reactor and the processing conditions.

References

[1] Dhanaraj, G., Huang, X. R., Dudley, M., Prasad, V., and Ma, R. H., *Crystal Growth Technology*, Springer, New York, 2003.

[2] Mehregany, M., Zorman, C. A., Rajan, N., and Wu, C. H., "Silicon Carbide MEMS for Harsh Environments," *Proceedings of the IEEE*, Vol. 86, No. 8, 1998, pp. 1594–1610. doi:10.1109/5.704265

[3] Mehran, M., and Christian, A. Z., "Silicon Carbide Micro- and Nanoelectromechanical Systems," *Proceedings of SPIE: The International Society for Optical Engineering*, Vol. 5342, SPIE—The International Society for Optical Engineering, Bellingham, WA, 2004, pp. 1–7.

[4] Wagner, G., Schulz, D., and Siche, D., "Vapour Phase Growth of Epitaxial Silicon Carbide Layers," *Progress in Crystal Growth and Characterization of Materials*, Vol. 47, Nos. 2–3, 2003, pp. 139–165. doi:10.1016/j.pcrysgrow.2005.01.001

[5] Dollet, A., de Persis, S., Pons, M., Matecki, M., "Simulation of SiC Deposition from $SiH_4/C_3H_8/Ar/H_2$ Mixtures in a Cold-Wall CVD Reactor," *Surface and Coatings Technology*, Vol. 177, Jan. 2004, pp. 382–388. doi:10.1016/j.surfcoat.2003.09.032

[6] Vorob'ev, A. N., Karpov, S. Y., Bogdanov, M. V., Komissarov, A. E., Bord, O. V., Zhmakin, A. I., and Makarov, Y. N., "Numerical Study of SiC CVD in a Vertical Cold-Wall Reactor," *Computational Materials Science*, Vol. 24, No. 4, 2002, pp. 520–534. doi:10.1016/S0927-0256(02)00220-3

[7] Rupp, R., Wiedenhofer, A., Friedrichs, P., Peters, D., Schorner, R., and Stephani, D., "Growth of SiC Epitaxial Layers in a Vertical Cold Wall Reactor Suited for High Voltage Applications," *Materials Science Forum*, Vol. 264, No. 2, 1998, pp. 89–96.

[8] Allendorf, M. D., and Kee, R. J., "A Model of Silicon-Carbide Chemical Vapor Deposition," *Journal of the Electrochemical Society*, Vol. 138, No. 3, 1991, pp. 841–852. doi:10.1149/1.2085688

[9] Danielsson, O., Henry, A., and Janzen, E., "Growth Rate Predictions of Chemical Vapor Deposited Silicon Carbide Epitaxial Layers," *Journal of Crystal Growth*, Vol. 243, No. 1, 2002, pp. 170–184. doi:10.1016/S0022-0248(02)01486-0

[10] La Via, F., Galvagno, G., Foti, G., Mauceri, M., and Veneroni, A., "4H SiC Epitaxial Growth with Chlorine Addition," *Chemical Vapor Deposition*, Vol. 12, Nos. 8–9, 2006, pp. 509–515. doi:10.1002/cvde.200506465

[11] Veneroni, A., and Masi, M., "Gas-Phase and Surface Kinetics of Epitaxial Silicon Carbide Growth Involving Chlorine-Containing Species," *Chemical Vapor Deposition*, Vol. 12, Nos. 8–9, 2006, pp. 562–568. doi:10.1002/cvde.200606468

[12] Chung, H. J., Polyakov, A. Y., Huh, S. W., Nigam, S., Skowronski, M., Fanton, M. A., Weiland, B. E., and Snyder, D. W., "Bulk Growth of High-Purity 6H-SiC Single Crystals by Halide Chemical-Vapor Deposition," *Journal of Applied Physics*, Vol. 97, No. 8, 2005, Paper 084913.

[13] Nigam, S., Chung, H. J., Polyakov, A. Y., Fanton, M. A., Weiland, B. E., Snyder, D. W., and Skowronski, M., "Growth Kinetics Study in Halide Chemical Vapor Deposition of SiC," *Journal of Crystal Growth*, Vol. 284, Nos. 1–2, 2005, pp. 112–122. doi:10.1016/j.jcrysgro.2005.06.027

[14] Dhanaraj, G., Dudley, M., Chen, Y., Ragothamachar, B., Wu, B., and Zhang, H., "Epitaxial Growth and Characterization of Silicon Carbide Films," *Journal of Crystal Growth*, Vol. 287, No. 2, 2006, pp. 344–348. doi:10.1016/j.jcrysgro.2005.11.021

[15] Chen, Y., Dhanaraj, G., Chen, H., Dudley, M., and Zhang, H., "Chemical Vapor Deposition and Defect Characterization of Silicon Carbide Epitaxial Films," *Materials Research Society Symposium*, Vol. 891, Materials Research Society, Warrendale, PA, 2006, Paper 891-EE12-11.

[16] Dhanaraj, G., Chen, Y., Chen, H., Cai, D., Zhang, H., and Dudley, M., "Chemical Vapor Deposition of Silicon Carbide Epitaxial Films and Their Defect Characterization," *Journal of Electronic Materials*, Vol. 36, No. 4, 2007, pp. 332–339. doi:10.1007/s11664-006-0084-2

[17] Fanton, M., Snyder, D., Weiland, B., Cavalero, R., Polyakov, A., Skowronski, M., and Chung, H., "Growth Of Nitrogen-Doped SiC Boules by Halide Chemical Vapor Deposition," *Journal of Crystal Growth*, Vol. 287, No. 2, 2006, pp. 359–362. doi:10.1016/j.jcrysgro.2005.11.044

[18] Pedersen, H., Leone, S., Henry, A., Beyer, F. C., Darakchieva, V., and Janzén, E., "Very High Growth Rate of 4H-SiC Epilayers Using the Chlorinated Precursor Methyltrichlorosilan (Mts)," *Journal of Crystal Growth*, Vol. 307, No. 2, 2007, pp. 334–340. doi:10.1016/j.jcrysgro.2007.07.002

[19] Wang, R., and Ma, R. H., "Kinetics of Halide Chemical Vapor Deposition of Silicon Carbide Film," *Journal of Crystal Growth*, Vol. 308, No. 1, 2007, pp. 189–197. doi:10.1016/j.jcrysgro.2007.07.038

[20] Bird, R. B., Stewart, W. E., and Lightfoot, E. N., *Transport Phenomena*, Wiley, New York, 1960.

[21] CHEMKIN, Software Package, Ver. 4.1, Reaction Design, San Diego, CA, 2006.

[22] Grujicic, M., and Cao, G., "Reactor Length-Scale Modeling of Chemical Vapor Deposition of Carbon Nanotubes," *Journal of Material Science and Technology (Sofia)*, Vol. 38, No. 8, 2003, pp. 1819–1830.